How to infer non-Abelian statistics and topological visibility from tunneling conductance properties of realistic Majorana nanowires

S. Das Sarma, Amit Nag, and Jay D. Sau
Condensed Matter Theory Center and Joint Quantum Institute and Station Q Maryland, Department of Physics, University of Maryland, College Park, Maryland 20742-4111, USA
(Received 31 March 2016; revised manuscript received 24 June 2016; published 20 July 2016)

We consider a simple conceptual question with respect to Majorana zero modes in semiconductor nanowires: can the measured nonideal values of the zero-bias-conductance-peak in the tunneling experiments be used as a characteristic to predict the underlying topological nature of the proximity induced nanowire superconductivity? In particular, we define and calculate the topological visibility, which is a variation of the topological invariant associated with the scattering matrix of the system as well as the zero-bias-conductance-peak heights in the tunneling measurements, in the presence of dissipative broadening, using precisely the same realistic nanowire parameters to connect the topological invariants with the zero-bias tunneling conductance values. This dissipative broadening is present in both (the existing) tunneling measurements and also (any future) braiding experiments as an inevitable consequence of a finite braiding time. The connection between the topological visibility and the conductance allows us to obtain the visibility of realistic braiding experiments in nanowires, and to conclude that the current experimentally accessible systems with nonideal zero-bias conductance peaks may indeed manifest (with rather low visibility) non-Abelian statistics for the Majorana zero modes. In general, we find that a large (small) superconducting gap (Majorana peak splitting) is essential for the manifestation of the non-Abelian braiding statistics, and in particular, a zero-bias conductance value of around half the ideal quantized Majorana value should be sufficient for the manifestation of non-Abelian statistics in experimental nanowires. Our work also establishes that as a matter of principle the topological transition associated with the emergence of Majorana zero modes in finite nanowires is always a crossover (akin to a quantum phase transition at finite temperature) requiring the presence of dissipative broadening (which must be larger than the Majorana energy splitting in the system) in the system. For braiding, this dissipation is supplied by the finite speed of the braiding process itself, which must be diabatic in any real experiment for braiding to succeed.

DOI: 10.1103/PhysRevB.94.035143

I. INTRODUCTION

In 2012, in an important experimental report [1], Mourik *et al.* presented evidence for the possible existence of non-Abelian Majorana zero modes (MZMs) in InSb nanowires subjected to an external magnetic (Zeeman) field in proximity to an ordinary *s*-wave superconductor (NbTiN in Ref. [1]). This experiment followed precisely earlier theoretical predictions [2–6] on how to create, localize, and observe MZMs in nanowires by judiciously combining Rashba spin-orbit coupling, Zeeman spin splitting, and *s*-wave superconducting proximity effect—the basic idea of the prediction, first explicitly developed in Ref. [2], being that a combination of spin-orbit coupling and spin splitting could, in principle, convert ordinary *s*-wave superconductors into topological (effectively spinless, although spin could play an important role in some situations [7]) *p*-wave superconductors which would carry localized MZMs at suitable defect sites (including the boundaries) provided the Zeeman field is large enough to overcome the *s*-wave superconducting gap, thus inducing a chiral [2,5] (or helical [3,6]) topological *p*-wave gap. The observation by Mourik *et al.* received considerable support from several other independent experiments [8–13] in semiconductor nanowires (both InSb and InAs) where signatures for the existence of MZMs were reported by other groups. The fact that a spinless *p*-wave superconducting wire would have localized MZMs (with non-Abelian anyonic braiding statistics) at the wire ends was already pointed out by Kitaev almost 15 years ago [14], and Sengupta *et al.* [15], also 15 years ago by coincidence, established the possibility that these MZMs, localized as zero-energy midgap interface states in topological superconductors, could be experimentally detected using differential tunneling spectroscopy where the perfect Andreev reflection associated with the MZMs would produce a quantized zero-bias conductance (precisely at zero energy, i.e., at midgap) which would be a signature of their existence. A similar signature for Majorana fermion edge states at the interface of a superconductor and surface of a topological insulator was made by Law *et al.* [16]. Such zero-bias conductance peaks (ZBCP), also predicted in the specific context of the semiconductor nanowires by Sau *et al.* [5], are precisely the observations of most of the experimental claims [1,8–13] for the possible observation of MZMs in semiconductor nanowires. The subject has created enormous excitement in the community because of the novelty associated with topological superconductivity and non-Abelian statistics as well as the possibility of carrying out fault-tolerant topological quantum computation using MZMs [17], and has been extensively reviewed in the recent literature [18–24]. The current work provides a link between the experimentally observed ZBCP in the semiconductor nanowires and the possible topological properties of the underlying MZMs through extensive numerical simulations calculating certain topological invariants along with ZBCP values for the same nanowire parameters.

Although the MZM interpretation (i.e., the relevant semiconductor nanowires in these experiments carry non-Abelian MZMs at the ends of the wires) is the most natural explanation for the experimental observations [1,8–13] in the

semiconductor nanowires, particularly in view of the existing theoretical predictions [2–6] preceding the experiments, many questions remain, and the possibility that the ZBCPs arise from some other nontopological mechanism cannot definitively be ruled out. In this regard, several mechanisms have been suggested, which do not necessitate the occurrence of a topological phase transition (TPT) for the appearance of ZBCP [25–31]. None of these alternate nontopological mechanisms requires the ZBCP to be canonically quantized to $2e^2/h$ as is the expected ideal value for the perfect Andreev reflection associated with MZMs [15,16,32,33]. However, the observed ZBCP in the experiments is not quantized either and is, in fact, typically well below $2e^2/h$, which has been explained as arising from a number of physical mechanisms affecting the experimental situation [34]. Several experimentally observed features of the ZBCP fall short of the idealized theoretical expectations: (1) ZBCP height is much smaller than the predicted perfect quantized value of $2e^2/h$; (2) recent attempts to produce ZBCPs closer to the quantized value typically appear to lead to a a broadening much larger than the thermal value [35]; and (3) ZBCP often does not manifest the expected oscillatory peak splitting (with increasing Zeeman field) predicted for MZMs [36–39] in finite length wires where the MZMs at the two wire ends should overlap with each other producing an energy splitting around zero bias. In spite of a large number of theoretical investigations in the literature, explaining the observed nonideal ZBCP properties as a result of underlying Majorana modes and its interplay with disorder, temperature, lead couplings and other nonidealities [16,34,40–45], it is hard to discount alternate nontopological mechanisms conclusively yet, particularly since the experimentally observed ZBCP remains well below the ideal quantized value of $2e^2/h$. At best, the experiments seem to (weakly) satisfy the necessary conditions for MZMs (i.e., the observation of a ZBCP under the predicted conditions), but not the sufficient conditions for claiming conclusive evidence supporting the existence of non-Abelian MZMs. It is entirely possible, perhaps even likely, that the invariable existence of finite disorder, finite temperature, finite wire length, finite coupling to the tunneling leads, imperfect proximity coupling, and other nonidealities in the realistic systems make it completely impossible to observe the predicted perfect ZBCP quantization of $2e^2/h$ in the experimental setups. It is encouraging that recent materials improvements in making the nanowires have led to a substantial enhancement in the observed value of the ZBCP although it is still smaller than the perfect quantized value of $2e^2/h$ [46]. However, it should be noted that zero-bias tunneling conductance peaks could arise in superconductors from a multitude of reasons, and cannot by itself be taken as compelling evidence for the existence of MZMs. We need some direct evidence for the topological phase transition accompanying the emergence of MZMs [47,48] and some measurements for topological properties. Perhaps the controversy regarding the existence or not of MZMs in nanowires would not arise if every experimental detection of the ZBCP found a value close to the expected universal quantized Majorana value of $2e^2/h$, but the fact that the experimental ZBCP value is both nonuniversal from experiment to experiment and is always much lower than $2e^2/h$ casts a dark shadow on the MZM interpretation of the experimental tunneling transport measurements.

Given that the defining exclusive property of the MZMs is their topological non-Abelian braiding characteristics [49,50] with the MZMs being subgap zero-energy non-Abelian anyonic excitations, it would seem that an experiment conclusively establishing their non-Abelian character would be the decisive sufficient condition for their existence. Indeed, several proposals have been put forth in the literature for probing the non-Abelian braiding properties of MZMs [24,51–65], and experimental efforts are currently underway to carry out MZM braiding to test their non-Abelian properties. An observation of the non-Abelian braiding properties would go a long way in establishing the existence of true MZMs in nanowires. The current work is a theoretical attempt to directly test what such a non-Abelian braiding experiment is likely to observe in realistic nanowires where the ZBCP is very far from being quantized and has large broadening. We establish in this work a clear connection between the observation of imperfect ZBCP and underlying topological properties, showing that the current experimental observations are indeed (but only marginally so) consistent with the possibility of the nanowires hosting non-Abelian Majorana zero modes purely from the perspective of braiding-related topological properties.

To provide a context, we start by assuming that the experimental observation in Ref. [1] (and other nanowire experiments) of the ZBCP is indeed a signature of (highly) imperfect MZMs which, because of various nonidealities in the system (e.g., disorder, temperature, tunnel coupling to the environment, finite wire length, Majorana splitting, etc.), produce a ZBCP, which is highly suppressed (and broadened) compared to the canonically quantized value of $2e^2/h$ [16,34,40,42,44]. The immediate question then is whether (or perhaps, to what extent) such imperfect almost-MZMs would have intrinsic non-Abelian braiding properties possibly showing up experimentally (or numerically in our study). In the absence of a braiding experiment to directly observe non-Abelian statistics for Majorana exchange at present, we are left to speculate on the extent to which non-Abelian statistics would be observed when nanowire MZMs are braided based on the only available experimental signal for their existence, i.e., ZBCP. It is then prudent to ask if we can relate the observed (nonideal) characteristics of the ZBCP, i.e., height and width of the peak, to the topological content of the approximate MZMs. Our work quantitatively establishes this connection and hence sheds light on the possibility of observing the topological nature of MZMs (in terms of non-Abelian exchange statistics) in future braiding experiments carried out in the same (or similar) samples as the ones currently manifesting nonideal ZBCPs. Thus, rather than simulating a future braiding experiment, we look at the electron tunneling properties of the nanowire close to zero energy to answer the extent to which it might be possible to demonstrate the non-Abelian characteristics of the Majorana modes for the given set of physical quantities of the system, viz., Majorana splitting, topological gap, tunneling strength, etc.

Kitaev suggested calculating a precisely defined quantity—topological invariant (TI)—to distinguish between trivial and topological phases in a p-wave superconducting wire [14]. The invariant suggested by Kitaev is suitable for systems with periodic boundary conditions. An appropriate generalization

of the TI suitable for a finite system with an open boundary condition was introduced by Akhmerov *et al.* [66] in terms of the S matrix of the associated system. Since we want to relate features observed in tunneling experiments (which are necessarily conducted on finite wires with open boundary conditions) to the underlying topological nature of the MZMs, we would use the proposed scattering matrix invariant to calculate the TI of the realistic system in order to quantify the topological nature of the semiconductor nanowire as we tune the physical parameters that are critical to the existence of MZMs, viz., wire length and Zeeman field. In fact, a variant of the scattering matrix TI were recently used in part by Adagedeli *et al.* [67] to show the existence of topological phase for disordered (mean free path $L_{\rm mf}$ shorter than the induced coherence length ξ) semiconductor nanowires.

However, a subtlety of the usual definition of the TI $Q_0 = \text{sgn}[\det(r)]$, where r is the reflection matrix from the end is that it requires us to ignore transmission of quasiparticles in-between the ends of the wire [66–68]. Such transmission of quasiparticles always exist for the finite wires we consider in this work. In fact, as we will discuss in more detail in this work, for finite wires the TI Q_0 is always trivial when one uses the exact reflection matrix (as opposed to the effectively semi-infinite approximation used in Refs. [66,67]). In this work, instead of ignoring transmission across the wire, we circumvent this problem by introducing dissipation into the system. While some form of dissipation has been important in previous calculations of the scattering matrix TI [67,68], dissipation in our work represents the finite rate of braiding. As pointed out in previous works [31,69] dissipation can change the qualitative behavior of Majorana modes and the TI.

The standard scattering TI Q_0 is not sensitive to imperfections of the topological phase such as transmission of quasiparticles through the wire. Such transmission through the wire would interfere with topological signatures of Majorana modes such as conductance quantization and non-Abelian statistics. To remedy this, we define a variant of the TI, $Q = \det(r)$, which we refer to as topological visibility (TV), as a measure of the topological character of the system. From the calculations presented here, it will become clear that the TV is better suited to determining the visibility of signatures of the Majorana fermion such as quantized conductance peak and non-Abelian statistics than the TI, which is just the sign of the TV. In the limit that we ignore transmission through the wire so that r is unitary, which is the case considered in Refs. [66–68], this quantity is identical to Q_0. One might be concerned that the topological visibility Q is not quantized as Q_0. However, Q is quantized as long as the system is properly gapped so that r is unitary. Whenever Q is not quantized, which is near a topological phase transition, whether Q_0 is trivial or not depends on nonuniversal details of the system which determine whether $\det(r)$ is slightly positive or slightly negative. To keep our terminology consistent with previous works [66–68], we will refer to $Q < 0$ to be topological [i.e., $Q_0 = \text{sgn}(Q) = -1$] and $Q > 0$ to be nontopological. The presence of dissipation eliminates the discreteness of the topological visibility Q by relaxing the unitarity of the theory, leading to the possibility of the TV being any number between $+1$ and -1 instead of having a magnitude precisely equal to unity. Only when Q is close to it's extreme values ± 1 can Q_0 be reliably determined to be topological or not. The competition between the strength of dissipation and the finite size splitting of Majorana modes in determining the TV is the central focus of our work. In fact, our work establishes that the emergence of MZMs in any finite length wires (i.e., in any experimental system, which must always use finite wires) is always a "topological quantum crossover" rather than a "topological quantum phase transition" where dissipative broadening plays a fundamental role—rather trivially, there is no topological phase in the absence of broadening in any finite length wire since the MZMs are never precisely at zero energy in finite wires! The TV of the finite system taking on any possible value between $+/-1$ rather than being precisely equal to $+1$ (nontopological) or -1 (topological) is a direct consequence of the topological transition being a crossover in the finite system with broadening—without any broadening, the finite system must always by definition have a TV equal to 1 since the MZM is always displaced from the energy zero. We identify the topological crossover point as the TV passing through zero in our calculation with the TV $<$ ($>$) 0 being identified as the topological (nontopological) phase. We also identify the deviation in the magnitude of the TV from unity being the direct manifestation of finite "visibility" in the braiding experiment—closer the TV is to unity in magnitude, higher is the visibility for the corresponding phase (depending on whether the TV is positive or negative).

The dissipation we introduce is not just a mathematical convenience and is an actual physical quantity present in the real experimental nanowires. Dissipation can play a role in reducing the conductance from the quantized Majorana value to the experimentally observed value (even at zero temperature). Similarly, dissipation might be responsible for increasing the width of the zero-bias peak beyond the thermal width [35]. One might wonder if it is possible for the dissipative broadening to exceed temperature. In fact, coupling to a fermion bath can lead to such dissipation even at nearly zero temperature. Such a fermion bath can arise from subgap states at the semiconductor-superconductor interface generated by disorder in the superconductor [70]. While a finite array of such subgap states is usually coherent, the presence of weak interaction and temperature coupled to such subgap states can lead to decoherence of the fermions, turning such a large density of subgap states into a fermion bath. Alternatively such a fermion bath can arise from subgap states in vortices generated by the magnetic field.

We will relate the topological nature of MZMs calculated in the tunneling conductance setup to the non-Abelian braiding statistics of MZMs through the appropriate direct numerical calculations of both the ZBCP and TV magnitudes in realistic systems, establishing correlations among them. If the experimentally observed ZBCPs are indeed almost-MZMs (and not spurious effects arising from totally distinct mechanisms that have nothing to do with topological superconductivity), then our work would provide a useful guide for the expected visibility of a non-Abelian braiding experiment in real samples since we start by numerically calculating ZBCPs in the nanowires ensuring that the calculated ZBCP magnitudes are approximately consistent with experimental observations. Our work in fact encompasses two qualitatively distinct realistic aspects of the experimental situation. First, we establish the

quantitative connection between having a ZBCP strongly suppressed from the quantized $2e^2/h$ value and the topological content of the associated almost-MZMs, i.e., we investigate how suppressed the ZBCP could be from $2e^2/h$ and still manifest some topological character. Second, we investigate the deleterious effects of MZM splitting, which must invariably be present in all finite nanowires because of the overlap of the MZMs from the two ends, on the braiding properties (or more precisely, on the value of the TV, which distinguishes topological and trivial phases). The key concepts of dissipative broadening and realistic finite lengths of the nanowires hosting MZMs play crucial conceptual as well as quantitative roles in our theory.

The reason for focusing on the tunneling scenario is twofold. First, Majorana tunneling experiments have already been successfully conducted whereas the braiding experiments with nanowire Majorana are proposed future works. This allows us to work with known experimental parameters and check our tunneling conductance results against the existing data that are either published or in principle should be under present experimental reach. Therefore quantitative expectations about putative non-Abelian Majorana braiding experiment of the future can be drawn based upon the available data and present experiments on the tunneling conductance by relating both sets of results on the same system. Second, it is conceptually easier to characterize and computationally easier to numerically simulate electron tunneling into Majorana nanowires than a braiding operation. We point out that ramifications of braiding operations on MZMs in an experiment have been studied theoretically and many detailed effects and subtleties have been pointed out in Refs. [71–76]. However, since we are focusing on the topological content of stationary Majorana modes (probed numerically by simulating a tunneling conductance measurement), our result would represent the best possible outcome one may hope to get towards observing the non-Abelian braiding statistics of MZMs. In particular, our work specifically connects the outcome of a braiding experiment (i.e., the direct measurement of the TV in a system) in relation to the measurement of the tunneling conductance in the same sample, answering the question whether a given value of a measured (in our case, numerically) ZBCP value is consistent or not with a topological value for the (numerically calculated) TV. In general, the non-Abelian character in a Majorana braiding experiment will be observed for fast enough braiding operation so that the energy uncertainty associated with the braiding time is larger than the Majorana splitting, which will entail approximate Majorana modes to appear to be roughly degenerate (as opposed to being well-split). However the experiment must distinguish the Majorana modes from the continuum set of (above-gap) bulk states. Therefore the speed of the braiding must be slow enough so that the associated energy uncertainty is not of the order of the topological gap. Or in other words, the braiding operation should be slow with respect to the inverse topological gap, but fast compared with the Majorana splitting. We argue that this is in complete analogy to how dissipative broadening, which is likely present in a tunneling conductance setup, must be larger than Majorana splitting but smaller than the topological gap to realize a nearly quantized conductance peak and also a topologically nontrivial value for the TV. Our detailed numerical simulations quantify these conceptual points. In fact, our work clearly establishes that one can make quantitative statements about "how topological" a particular system could be (at least, the upper bound) based simply on a detailed knowledge of the ZBCP peak height and broadening.

In this work we explore the connection between conductance and the TV and calculate their dependence on the Majorana splitting and the energy gap. These effects are studied for a specific Majorana hosting semiconductor Rashba nanowire (e.g., InSb or InAs nanowire with strong Rashba spin-orbit coupling) model proposed by Lutchyn *et al.* and Oreg *et al.* [3,6]. This particular model benefits from having been studied extensively theoretically (especially see Refs. [41,77]) as well as from being used as the theoretical guide to realize MZMs experimentally [1]. The paper is organized as follows. In Sec. II, we introduce the model Hamiltonian and write it in its discretized form to make it amenable to numerical techniques. In Sec. III, we investigate the effect of relevant energy scales, namely Majorana splitting and broadening, on the behavior of the TV and conductance near the topological phase transition as well as deep in the topological phase. Particular emphasis is placed on possible correlations between the two quantities in this general set-up. In Sec. IV, we use the relationship between braiding, tunneling conductance, and TV to study how conductance measurements can be used to characterize the outcomes of braiding experiments. Finally, we conclude in Sec. V. Appendix A reviews the details of calculating the conductance and TV from the scattering matrix for the nanowire model obtained using KWANT [78]. In Appendix B, we discuss some more technical subtleties that arise in the numerical calculations using the S matrix leading to the TV.

II. MODEL HAMILTONIAN

A schematic representation for an experimental setup to measure tunneling conductance is shown in Fig. 1. A semiconductor nanowire with Rashba spin-orbit coupling (SOC) is attached to a normal lead through a potential barrier localized at the end. A magnetic field is applied parallel to the wire (perpendicular to the SOC direction) and an s-wave superconductor is placed in proximity to the nanowire to facilitate Cooper pair tunneling into the semiconductor effectively

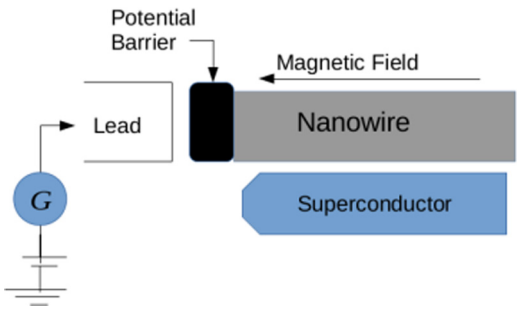

FIG. 1. A schematic diagram for measuring the tunneling conductance. One end of the Rashba nanowire is shown attached to a normal lead. The lead is connected to the nanowire through a potential barrier. Magnetic field is parallel to the nanowire. Proximate s-wave superconductor is responsible for the superconducting order parameter in the nanowire.

endowing the nanowire with an s-wave superconducting order parameter through proximity coupling. A voltage bias V is applied to the lead and the tunneling current I is measured to obtain the differential conductance

$$G = dI/dV. \tag{1}$$

As discussed in more detail in the appendix, for N conducting channels in the lead, the conductance G can be computed from the normal reflection matrix r_{ee} and the Andreev reflection matrix r_{eh} through the relation,

$$G = N - \mathrm{Tr}(r_{ee}r_{ee}^{\dagger} - r_{eh}r_{eh}^{\dagger}), \tag{2}$$

and the TV can be computed from the zero-frequency reflection matrices [66] as

$$Q = \mathrm{Det}[r_{ee}r_{ee}^{*} - r_{ee}r_{eh}r_{ee}^{-1}r_{eh}^{*}]. \tag{3}$$

The reflection matrices can be computed given the system and lead Hamiltonian, which we discuss in the remainder of the section.

Let us consider a particular semiconductor Rashba nanowire model introduced by Lutchyn *et al.* [3]—see also Refs. Sau *et al.* [2] and Oreg *et al.* [6]—which was shown to support MZMs at the two ends in the clean limit. These theoretical works directly motivated the nanowire Majorana experiments of Refs. [1,8–13]. The BdG Hamiltonian describing the 1D nanowire in the presence of Rashba SOC, Zeeman splitting, and superconducting proximity effect, is given by

$$H_{\mathrm{sys}} = \left(-\frac{1}{2m^*}\partial_x^2 + i\alpha_R\sigma_y\partial_x - \mu\right)\tau_z + \mu_0 B\sigma_x + \Delta_0\tau_x, \tag{4}$$

where, m^*, α_R, μ, and Δ_0 are the effective mass, the strength of Rashba SOC, the chemical potential and the proximity induced superconducting gap, respectively. Throughout this paper we set $\hbar = 1$. Here and henceforth $\tau_{x,y,z}$ and $\sigma_{x,y,z}$ are Pauli matrices acting on particle-hole and spin space, respectively. $\mu_0 = g\mu_B$ is the usual gyromagnetic ratio times the Bohr magneton defining the Zeeman field strength $\mu_0 B$. To make it amenable to numerical techniques, we discretize the continuum Hamiltonian as

$$\begin{aligned} H_{\mathrm{sys}}^{\mathrm{dis}} = \sum_{n=1}^{N}[&-t(|n+1\rangle\langle n| + \mathrm{H.c.})\tau_z \\ &+ i\alpha(|n+1\rangle\langle n| - \mathrm{H.c.})\sigma_y\tau_z + \Delta_0|n\rangle\langle n|\tau_x \\ &+ (-\mu+2t)|n\rangle\langle n|\tau_z + V_Z|n\rangle\langle n|\sigma_x], \end{aligned} \tag{5}$$

where $t = \frac{1}{2m^*a^2}$ with a being the lattice constant for the discretized tight-binding model in Eq. (5). Length of the nanowire is given by $L = aN$, where N is the number of unit cells in the wire, the SOC strength is given by $\alpha = \frac{\alpha_R}{2a}$, and we have defined the Zeeman field strength, $V_Z \equiv \mu_0 B$ giving the spin splitting. The nondiagonal terms in the site index arise from nearest neighbor hopping. This system has been shown to support MZMs [3,6]. In fact, for a clean nanowire it is now well-known that MZMs exist as stable localized zero-energy excitations at the ends of the nanowire whenever $V_Z > \sqrt{\Delta_0^2 + \mu^2}$.

Before we describe the normal leads that attach to the nanowire to create the normal-superconductor (NS) junction (see Fig. 1) for tunneling measurements, we first comment on an important quantity that can be calculated from the system Hamiltonian. It is known that MZMs contribute a local density of states (LDOS) zero-bias peak in the topological phase [41]. LDOS not only probes the presence of zero-energy modes, but also whether the zero-energy mode is localized close to the edge of the wire. In fact, computing or measuring the LDOS is the simplest probe to test the presence or absence of MZMs in the system. LDOS at a given energy ϵ and site i is given by

$$\begin{aligned} \mathrm{LDOS}(\epsilon,i) = \sum_n &(|u_{n\uparrow}(i)|^2 + |u_{n\downarrow}(i)|^2 \\ &+ |v_{n\uparrow}(i)|^2 + |v_{n\downarrow}(i)|^2)\delta(\epsilon - \epsilon_n), \end{aligned} \tag{6}$$

where $\psi_n(i) = (u_{n\uparrow}(i), u_{n\downarrow}(i), v_{n\uparrow}(i), v_{n\downarrow}(i))^T$ is the ith component of eigenvector ψ_n of the Hamiltonian matrix $H_{\mathrm{sys}}^{\mathrm{dis}}$ with eigenvalue ϵ_n. u's and v's are eigenvector components in particle and hole space, respectively. To calculate the tunneling conductance, we must attach leads to the Rashba nanowire. We assume the leads to be translationally invariant semi-infinite normal leads. The lead Hamiltonian is given by

$$H_{\mathrm{lead}} = \left(-\frac{1}{2m^*}\partial_x^2 + i\alpha_R\sigma_y\partial_x - \mu_{\mathrm{lead}}\right)\tau_z + \mu_0 B_{\mathrm{lead}}\sigma_x. \tag{7}$$

The above lead Hamiltonian is discretized as

$$\begin{aligned} H_{\mathrm{lead}}^{\mathrm{dis}} = \sum_n [&-t(|n+1\rangle\langle n| + \mathrm{H.c.})\tau_z \\ &+ i\alpha(|n+1\rangle\langle n| - \mathrm{H.c.})\sigma_y\tau_z \\ &+ (2t - \mu_{\mathrm{lead}})|n\rangle\langle n|\tau_z + \mu_0 B_{\mathrm{lead}}|n\rangle\langle n|\sigma_x]. \end{aligned} \tag{8}$$

Following the Delft experiment [1], a finite applied magnetic field B_{lead} is assumed to exist so as to have two nondegenerate conducting channels because of the spin splitting induced by B_{lead}. Having a finite magnetic field in the lead also helps us to avoid the numerical challenge to identify and separate various channels to compute the S matrix. We emphasize, however, that our keeping a finite B_{lead} is actually consistent with the experimental situation (and not just a matter of computational convenience).

The potential barrier defining the NS junction at the lead-nanowire interface (see Fig. 1) is simulated by modulating the hopping amplitude t' between the nanowire and the lead. For higher (lower) tunnel barrier, the hopping amplitude t' is lower (higher). The new system Hamiltonian $H_{\mathrm{sys}}^{\mathrm{dis}} \longrightarrow H_{\mathrm{sys}}^{'\mathrm{dis}}$ has the form

$$\begin{aligned} H_{\mathrm{sys}}^{'\mathrm{dis}} = \sum_{n=2}^{N}[&-t(|n+1\rangle\langle n| + \mathrm{H.c.})\tau_z \\ &+ i\alpha(|n+1\rangle\langle n| - \mathrm{H.c.})\sigma_y\tau_z \\ &+ (-\mu+2t)|n\rangle\langle n|\tau_z \\ &+ V_Z|n\rangle\langle n|\sigma_x + \Delta_0|n\rangle\langle n|\tau_x] \\ &- \left(t'|2\rangle\langle 1| + \mathrm{H.c.}\right)\tau_z + i\alpha'(|2\rangle\langle 1| - \mathrm{H.c.})\sigma_y\tau_z \\ &+ (2t - \mu_{\mathrm{lead}})|1\rangle\langle 1|\tau_z + \mu_0 B_{\mathrm{lead}}|1\rangle\langle 1|\sigma_x. \end{aligned} \tag{9}$$

In this setup, t' and α' correspond to hopping and spin-orbit coupling between the lead and the nanowire, respectively. $t' \ll t$ would correspond to a high tunnel barrier or weak lead-nanowire coupling. When $t' \sim t$, the tunnel barrier is low or equivalently, the lead-nanowire coupling is strong (i.e., the barrier is almost transparent). The lead-nanowire tunneling t' introduces a broadening (Γ_L) to be discussed later in the paper [cf. Eq. (11)]. A strongly coupled (i.e., large t') lead-nanowire system will have strongly broadened conductance peaks, whereas a weakly coupled lead-nanowire system will have weakly broadened sharp peaks. Narrow resonances appearing from states that are weakly coupled to the lead (as a result of being localized far away from the end) are removed by broadening the energy eigenstates by introducing an on-site imaginary term in the Hamiltonian, i.e., $H'^{\rm dis}_{\rm sys} \longrightarrow H'^{\rm dis}_{\rm sys} + b$, where

$$b = \sum_{n=2}^{N} (-Ji)|n\rangle\langle n|\mathbb{1}. \tag{10}$$

Here, J is the parameter controlling the intrinsic broadening, Γ, in the conductance profile. The two are related by, $\Gamma = 2J$. We note that this intrinsic broadening is again incorporated in the theory to be consistent with the experimental situation (and not just for computational efficacy) since the measured tunneling conductance spectra do not reflect sharp resonant structures even at the lowest temperatures. Obviously, an environment-induced dissipative broadening (parametrized by Γ in our theory) plays a role in the experiment. We emphasize that broadening plays a key role in our theory converting the topological quantum phase transition into a crossover and providing a visibility for the braiding measurements.

LDOS is calculated by numerically diagonalizing the system Hamiltonian. Throughout all our calculations, the following set of parameters (unless specified otherwise) is used: $\alpha = 1.79$ K, $\mu = 0$ K, $t = 12.5$ K, $\Delta_0 = 3$ K, $L = 1.5$ μm, and $a = 54$ nm. For reasons motivating the choice of the parameter set, we refer the reader to Ref. [41]. We believe these parameters to be a reasonably realistic description of the experimental situation in Ref. [1], at least at a qualitative level. As discussed in Appendix A, the conductance and TV are calculated from the scattering matrix that is obtained using "KWANT"—a quantum transport and simulations package in Python developed principally by Groth *et al.* [78].

III. RESULTS: CONDUCTANCE AND TOPOLOGICAL VISIBILITY

A. Role of broadening versus splitting

While the TV and conductance will be determined by all the microscopic parameters discussed in the last section, we now argue that the qualitative behavior can be understood in terms of a few effective parameters, which in turn are determined by the full set of microscopic parameters in a simple way. For example, as seen from the calculated local density of states plotted in Fig. 2, one of the relevant scales that affects the topological properties, the splitting of the MZMs (δ), is relatively independent of the other scales such as lead coupling, but sensitively determined by small variations in the microscopic Zeeman field V_Z in an oscillatory fashion

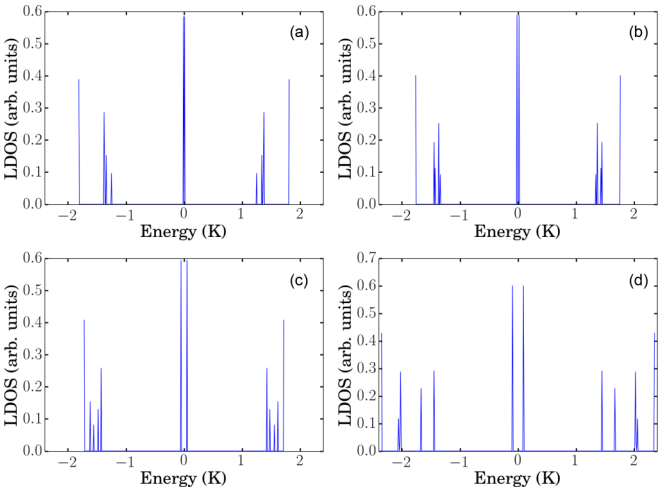

FIG. 2. LDOS for clean nanowire with $L = 1.5$ μm and Zeeman field strengths (a)–(d), $V_Z = 4.2, 4.3, 4.5$, and 5.0 K. The corresponding Majorana splitting (a)–(d) are $\delta = 0.012, 0.036, 0.094$, and 0.18 K respectively clearly vary strongly with V_Z.

[36–39]. We note that δ is a key parameter determining the topological content of the system in the sense that when this quantity is (exponentially) small, the system is by definition non-Abelian, whereas by contrast, when δ is comparable to the superconducting energy gap, the system is manifestly not topological.

The topological properties of a one-dimensional superconductor such as a semiconductor nanowire crucially depend on the various relevant sources of broadening, such as the lead coupling and inelastic scattering, of the quasiparticle excitations. The width of the ZBCP, which is a key signature of topological superconductivity, depends on the broadening, Γ_L, which is controlled by tuning the lead tunneling t' discussed in the previous section. Furthermore, the TV, Q, [66], which characterizes the topology of nanowires with open boundary conditions, is necessarily nontopological (i.e., $Q = 1$) [66] because any calculation of TV in the presence of finite δ (which must always be true in any finite wire) and no broadening must necessarily give $Q = 1$ (i.e., a nontopological trivial system) since the MZM is not located precisely at zero energy for any finite length wire! Typically, this is circumvented by computing the TI at an energy arbitrarily shifted slightly away from zero by the splitting of the MZM, δ. A similar behavior is noticed [34] in the low-bias conductance $G(V) = dI/dV$, which characterizes MZMs through a quantized value $G(V \to 0) = G_0 = 2e^2/h$ [15,16,32,33]. For a finite system, the conductance $G(V \gtrsim \delta)$ approaches the quantized value $G(\Gamma_L \gg V \gtrsim \delta) \to G_0$. On the other hand, as V truly approaches zero (i.e., $|V| \ll \delta$), the conductance in the tunneling limit approaches zero [34], giving a vanishing ZBCP (since the Majorana is not located precisely at zero energy in a finite length wire).

Therefore both the TV (Q) and the zero-bias conductance (G) cannot be evaluated strictly at zero-energy for a finite wire to determine the topological phase of the wire. In this work, motivated by the goal of understanding finite rate dynamical processes such as braiding, we avoid this problem by introducing an intrinsic quasiparticle decay rate

(i.e., dissipative broadening), Γ, which we believe to be the realistic experimental situation. The broadening Γ is controlled in our calculations by choosing the parameter J discussed in Sec. II. The introduction of such a scale allows us to discuss the conductance (G) and TV (Q) in a meaningful way at exactly zero energy. The intrinsic decay rate, Γ, apart from representing the uncertainty in energy resulting from the finite braiding rate, likely also exists in semiconductor wires from interactions and phonons (and unknown dissipative coupling to the environment invariably present in all solid state systems). Moreover, since the conductance and the TV are determined by the scattering properties of electrons from an external lead, the coupling to the lead, which is parametrized by the broadening Γ_L, quantitatively affects these topological properties. Finally, the superconducting gap Δ that protects topological properties themselves must play a role in determining the topological properties. In the following sections, we will study the interdependence of the conductance and the TV on these energy-scales, namely, δ, Γ, Γ_L, and Δ. We emphasize that the problem is highly complex because these are four completely independent energy scales (and in real experimental systems there are at least two additional energy scales associated with finite temperature and disorder neglected in the current work).

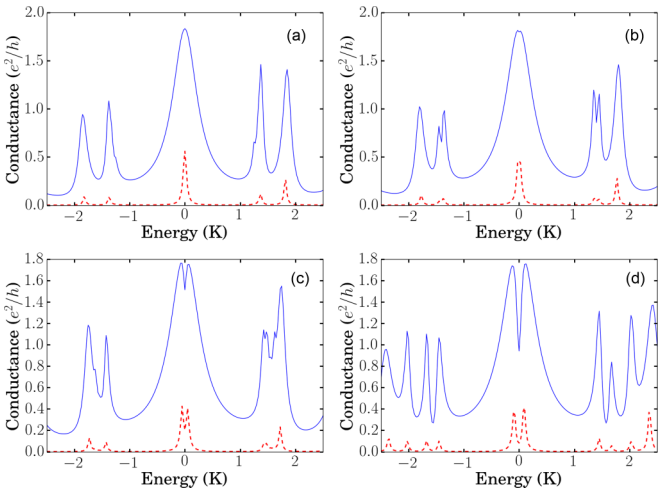

FIG. 3. Conductance plot corresponding to the LDOS splittings for $\Gamma_L/\Gamma = 10$ (blue solid curve) and 0.25 (red dashed curve). (a)–(d) The parameter $\delta/\Gamma = 0.27, 0.71, 1.74$, and 3.27, respectively. The TV (Q) values (a)–(d) are $(-0.80, -0.75, -0.46, 0.12)$ and $(0.44, 0.58, 0.82, 0.93)$ for blue solid and red dashed curves, respectively. The conductance peaks split for large δ/Γ and the conductance decreases for small Γ_L/Γ.

B. Topological phase

We start by discussing the zero-bias conductance and TV deep in the topological phase where the intrinsic quasiparticle broadening Γ is much smaller than the topological gap $\Delta \gg \Gamma$ so that the gap Δ is well-defined. We choose the nanowire to be sufficiently long, in this subsection, so that the Majorana splitting δ and the broadening of the MZMs from the lead are much smaller than the gap (i.e., $\delta, \Gamma_L \ll \Delta$).

Since the topological gap Δ is much larger than the parameters relevant to the MZMs namely, the splitting δ, the broadening of the MZM due to coupling to the lead, Γ_L, and the (intrinsic) broadening of the far end MZM (away from the lead), Γ, both the zero-bias conductance $G(V = 0)$ and the TV Q, is a function only of δ, Γ_L, and Γ. Note that the broadening of the MZM at the far end is the same as the intrinsic quasiparticle broadening Γ, since it is not coupled to the lead. Since the absolute energy scale cannot matter, the conductance $G(V = 0)$ and the TV, Q, can be studied as a function of dimensionless parameters Γ_L/Γ and δ/Γ (in this large Δ limit).

Consider first the limit where $\delta/\Gamma \gg 1$, i.e., the broadening is much smaller than the Majorana splitting. As seen from the conductance plot in Figs. 3(c) and 3(d) (red dashed curve), if the lead coupling also weak i.e., $\Gamma_L \ll \delta$, the conductance profile $G(V)$ shows a pair of resonances at energies $E = \pm\delta/2$ with broadening of order $(\Gamma + \Gamma_L)$. The height of these peaks would be substantially below the quantized value. As seen from the solid blue curve in Figs. 3(c) and 3(d) and consistent with previous work [34], increasing the lead coupling so that $\Gamma_L \gg \delta$, increases the height of the zero-energy peak so as to approach the quantized value $G(V \sim 0) \sim G_0$. However, the splitting δ now appears as a dip in the conductance, which reduces the conductance $G(V = 0)$ at strictly zero bias. Thus the zero-bias conductance $G(V = 0)$ is suppressed from the quantized value, and as expected from the connection between conductance and TV [33], we find the TV Q to be nontopological (i.e., positive in this parameter regime).

The conductance $G(V)$ in the opposite limit, where $\delta/\Gamma \ll 1$, is shown in Figs. 3(a) and 3(b) and shows an unsplit ZBCP. The conductance in the $\Gamma_L \gg \Gamma$ (blue curve) shows a nearly quantized conductance, while the conductance is suppressed in the opposite limit. However, this limit (i.e., $\Gamma_L \ll \Gamma$) (red dashed curve) still shows a ZBCP, albeit substantially smaller than the quantized value even though the corresponding TV is nontopological. On a technical note, varying the Zeeman field between the different panels in Fig. 3 changes Δ. To mitigate any parametric dependence of the calculated ZBCP and TV on Δ, in this subsection the broadening Γ is adjusted in each case to hold $\Delta/\Gamma = 52$ fixed (remembering that the gap Δ depends on the Zeeman field). The lead broadening Γ_L is varied through varying t' [see Eq. (11) below] to keep the ratio Γ_L/Γ fixed.

The TV is strongly affected by the splitting of the MZMs δ relative to the broadening Γ. In Fig. 4, we find that the TV is an increasing function of δ/Γ. The nanowire effectively becomes nontopological if the MZM splitting δ exceeds the broadening Γ, even when the wire parameters and the strong lead coupling Γ_L favor the topologically nontrivial phase. Furthermore, consistent with the conclusion in Fig. 3, the small values of Γ_L/Γ lead to nontopological values for the TV.

The combination of Figs. 3 and 4 suggests a correlation between the presence of a quantized ZBCP and a topologically nontrivial value of the TV close to $Q = -1$. This correlation between TV and conductance suggested by Figs. 3 and 4 is made explicit in Fig. 5. We find that TV is a decreasing function of the ZBCP value. The TV approaches $-1(+1)$ as ZBCP approaches $2e^2/h(0)$. Note that the decreasing behavior of TV with increasing ZBCP is independent of the tuning parameter chosen to vary the zero-bias conductance, evidenced by the fact

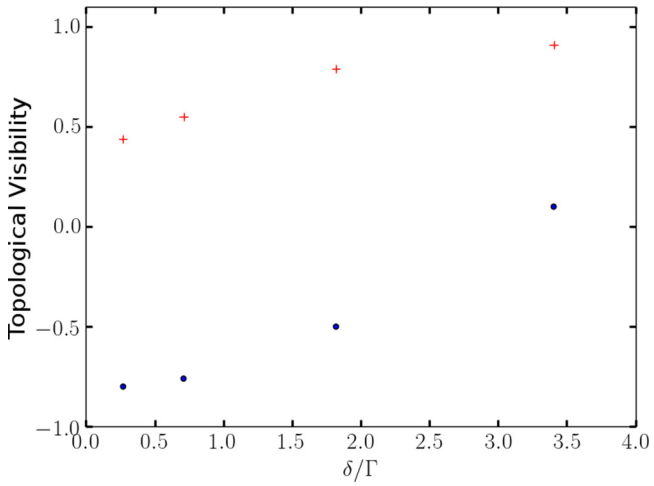

FIG. 4. TV for δ/Γ values corresponding to Fig. 3 for coupling parameter $\Gamma_L/\Gamma = 10$ (blue dots) and 0.25 (red plus). The TV is an increasing function of δ/Γ, i.e., the system tends to become nontopological as δ/Γ increases.

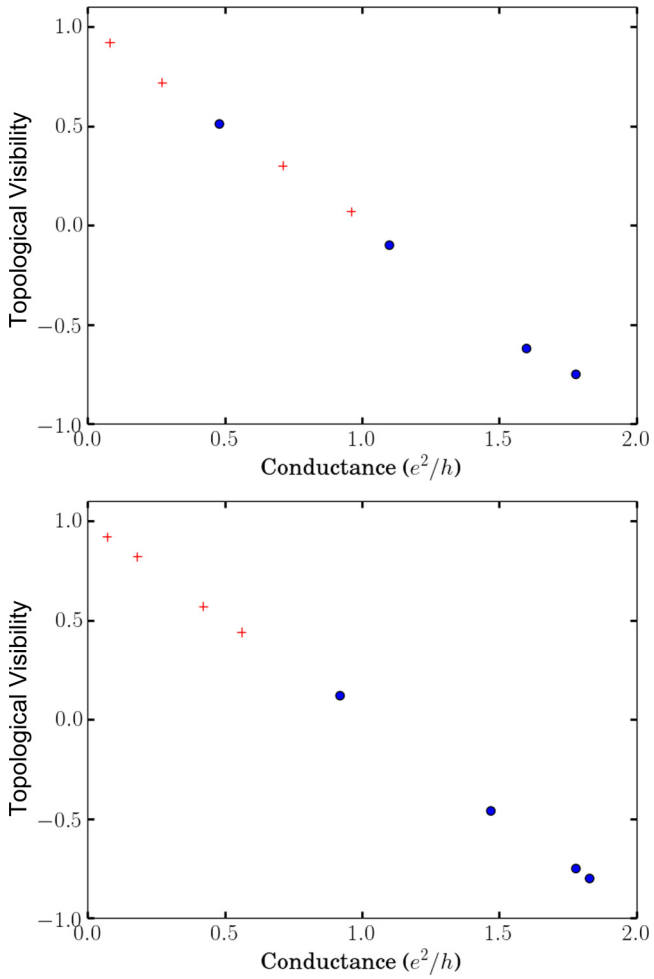

FIG. 5. (Top) Plot of the TV as a function of ZBCP for $\delta/\Gamma = 0.16$ (blue dot) and 2.43 (red plus). Conductance is varied by varying Γ_L/Γ. (Bottom) TV vs ZBCP for $\Gamma_L/\Gamma = 10$ (blue dot) and 0.25 (red plus). Conductance is varied by varying δ/Γ. The TV is a decreasing function of the ZBCP.

that both top and bottom plots in Fig. 5 manifest a decreasing behavior for the TV as a function of ZBCP regardless of whether Γ_L/Γ (top subfigure Fig. 5) or δ/Γ (bottom subfigure Fig. 5) is tuned to vary ZBCP.

C. Topological phase transition

Let us now consider the behavior of conductance and TV as we approach the TPT by tuning the Zeeman field V_Z. In this case, when the intrinsic broadening Γ and the lead-induced broadening Γ_L are small, sufficiently close to the phase transition, the topological gap Δ will become smaller than $\Delta \ll \Gamma$ (since at the TPT, the gap must vanish). Therefore, for infinite length systems, the ratio Δ/Γ can be used to determine the distance to the quantum critical point. For conventional quantum critical points [79], there are two dimensionless parameters that characterize the distance to a quantum critical point, which are L/ξ and Δ/T characterizing spatial and imaginary time correlations in the system. Here ξ is the coherence length of the system, Δ is an energy scale, T is the temperature, and L is the length of the system. In our discussion, Γ is analogous to temperature T in the quantum critical phase (although we are actually at $T = 0$ throughout). Since Γ is always finite in our system, the TPT is always a crossover even at zero temperature! The fact that our calculated TV value in Figs. 4 and 5 is continuous between $Q = +1$ (trivial phase) and $Q = -1$ (topological phase) is a clear indication that the presence of dissipative broadening in the theory (and the associated nonunitarity) has rendered the TPT into a crossover with $Q > (<)0$ defining the nontopological (topological) phase with finite visibility. The presence of dissipation makes some additional changes to the topological transition that we mention in passing. Traditionally in disordered systems the topological transition is often accompanied by a Griffiths like phase populated by weakly split low-energy Majorana modes [80]. The presence of dissipation could change some of these weakly split Majorana modes into poles of the now nonunitary S matrix with exactly zero energy but different imaginary parts [31]. Such physics, which is exactly included in our theory, would alter the nature of the low-energy density of states near the transition.

The relationship between Γ_L and Δ is not straightforward because as the system approaches the TPT, the bound states become delocalized away from the lead due to the diverging coherence length ξ. In the limit of small lead-tunneling, t', the broadening Γ_L induced by the lead is related to the imaginary part of the lead self-energy [81] and can be written as

$$\Gamma_L \sim t'^2 |\psi(0)|^2, \tag{11}$$

where $\psi(0)$ is the value of the nanowire wave function at the lead-nanowire NS contact at the given tunneling energy. The localized Majorana wave function can be approximated by

$$\psi(x) \approx \frac{1}{\sqrt{\xi}} e^{-x/\xi}, \tag{12}$$

where ξ is the superconducting coherence length. This implies

$$\Gamma_L \sim t'^2 \Delta. \tag{13}$$

Therefore, in the vicinity TPT, $\Delta/\Gamma_L \propto t'^2$ (with the proportionality factor related to the normal phase density of

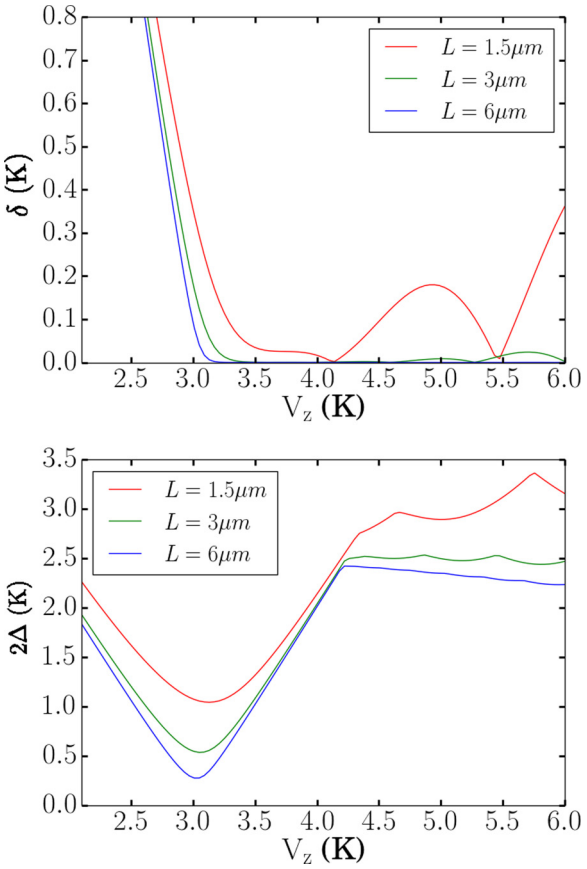

FIG. 6. Plot of the lowest Andreev bound state energy (top) and bulk quasiparticle energy gap (bottom) as a function of Zeeman field strength for different physical lengths of Majorana nanowire. The bulk TPT is at $V_Z = 3$ K. In the topological phase, ($V_Z > 3$ K), lowest Andreev bound state energy is the Majorana splitting.

states) approaches a constant and can be used as a parameter to characterize the TPT. Note that although Γ_L is in some sense proportional to the gap Δ, the two quantities are still independent parameters of the theory by virtue of the lead tunneling matrix element t'.

As seen in Fig. 6, the TPT is approached by tuning the Zeeman field V_Z, which leads to the variation of both the Majorana splitting δ (lowest Andreev bound state energy) in the upper panel and the bulk gap Δ (next highest Andreev bound state energy) in the lower panel. The minimum in the gap Δ occurs at $V_Z = 3$ K indicating a transition at this value of the Zeeman potential. For a finite system, the minimum gap is determined by the length of the system L. In the case where the wires are shorter than the dephasing length $l_\phi \sim v/\Gamma$ (for the chosen Γ), where v is the Fermi velocity of the system, the MZMs split before entering the TPT region $\Delta \lesssim \Gamma$. As a result, the system enters a nontopological phase with a TV close to $Q = 1$ similar to the $\delta \gtrsim \Gamma$ case discussed in the last subsection. Therefore, in this section, we focus on a broadening Γ that is larger than the finite size gap, i.e., $\Gamma \gtrsim v/L$.

Let us now consider the conductance shown in Fig. 7 as the Zeeman field is varied towards the topological transition. Figure 7(a) shows a nearly quantized peak (blue solid) deep in the topological phase where the MZM splitting δ is also

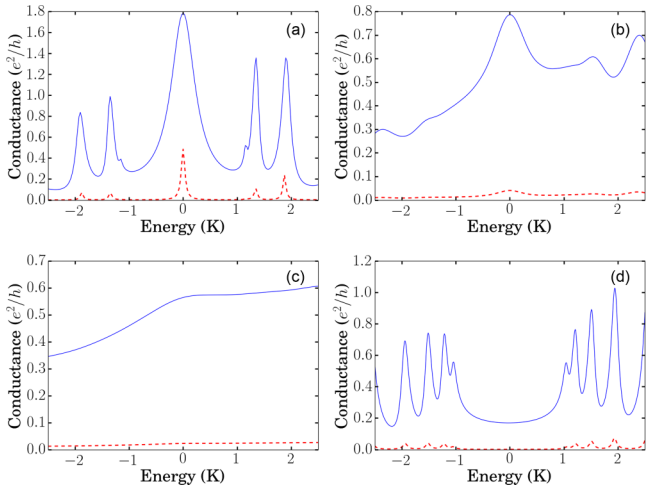

FIG. 7. Conductance plot for $\Gamma_L/\Delta = 0.20$ (blue solid curve) and 0.005 (red dashed curve). Broadening Γ is chosen so that $\delta/\Gamma = 0.16$ is held fixed for all panels with Δ/Γ (a)–(d) being 19.33, 0.90, 0.28, −12.1, respectively. The TV (Q) values (a)–(d) are (−0.75,0.34,0.56,0.98) and (0.51,0.95,0.97,1.0) for blue solid curve and red dashed curve, respectively.

small relative to the broadening Γ. The corresponding TV is also seen to be nearly topological in Fig. 8 as expected. As the Zeeman field is decreased, the height of the ZBCP (above the background) decreases as one approaches the topological transition where $\Delta/\Gamma \to \delta/\Gamma$ becomes small in Fig. 7(c). However, it should be noted that the peak remains unsplit in contrast to the short wire case with $L \lesssim l_\phi$. Despite the presence of a small zero-bias peak in Figs. 7(b) and 7(c), the corresponding TV values in Fig. 8 are positive (nontopological). This is consistent with Figs. 3 and 4 from the previous subsection where a small coupling $\Gamma_L \ll \Gamma$ led to

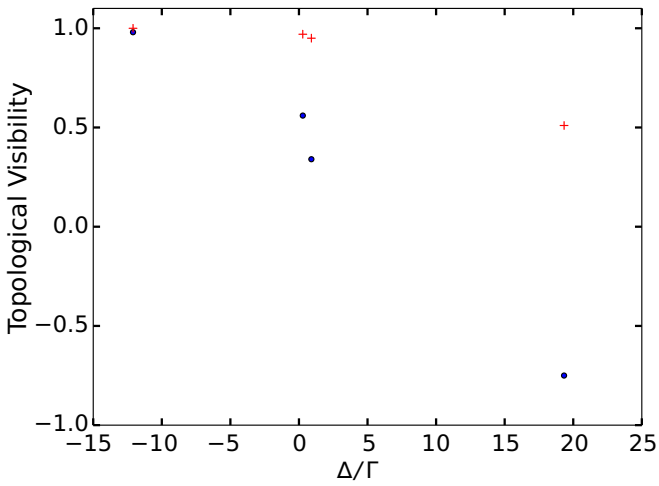

FIG. 8. TV for Δ/Γ values corresponding to Fig. 7 for coupling parameters near TPT with $\Gamma_L/\Delta = 0.20$ (blue dots) and 0.005 (red plus), respectively. $\delta/\Gamma = 0.16$ is held fixed. The TV is an decreasing function of Δ/Γ with $Q \longrightarrow 1$ as $\Delta/\Gamma \longrightarrow 0$, i.e., the system tends to become non-topological (topological) as the system tends to small (large) topological gap and the TV tends to +1 as the gap completely closes (system approaches TPT).

small nontopological ZBCP. Finally, as one crosses over to the nontopological regime, a nontopological gap appears in the conductance. As mentioned before, the TPT is parameterized by Γ_L/Δ, which remains relatively constant near the phase transition. The red dashed plots in Fig. 7 show that the conductance is systematically suppressed in the regime of small Γ_L/Δ. The corresponding TVs are seen to be positive (nontopological) in Fig. 8.

Before concluding this section, we comment on an obvious point, which might confuse a nonalert reader. One may think that the TV can have only unit magnitude with $Q = -1(+1)$ characterizing the topological (trivial) phase. This is indeed so in the infinite system as originally introduced by Kitaev. But our finite system must have a broadening (otherwise the TV calculated at zero energy is always $+1$ because of Majorana splitting), and this broadening allows the TV (i.e., Q) to be a continuous function of system parameters going from $+1$ deep in the trivial phase to -1 deep in the topological phase. This continuous evolution of Q between $+1$ and -1 is the finite system crossover transition whereas the corresponding infinite system would have a sharp transition from $+1$ to -1 precisely at the TPT (with the ZBCP value changing from zero to $2e^2/h$ sharply at the TPT too). The new idea in the current work is to connect this crossover transition to braiding experiments with the claim that our finding a value of $Q < 0$ corresponds to a topological phase with the visibility of the braiding measurements being large (small) depending on whether the magnitude of Q is close to unity (zero). We believe that our finding a negative (positive) value of Q corresponds to the corresponding braiding experiment manifesting (not manifesting) non-Abelian statistics.

IV. BRAIDING AND TUNNELING CONDUCTANCE

In a 1D system, MZMs appear as a pair of zero-energy modes (i.e., precisely at mid-gap assuming no Majorana splitting, i.e., no overlap between the two MZM wave functions) localized spatially at the two wire ends. N such pairs of localized MZMs form a 2^N dimensional degenerate zero-energy subspace within the Hilbert space of the system. A possible braiding process involving two MZMs via a so called trijunction [64] is depicted in Fig. 9. Let $\hat{\gamma}_{1,2}$ and $\hat{\gamma}'_{1,2}$ represent the Majorana operators, associated with the localized Majorana modes $\gamma_{1,2}$ and $\gamma'_{1,2}$ depicted in the Fig. 9(a). The ground state is initialized as a direct product state of left and right Majorana pairs, $|P_L\rangle_1|P_R\rangle_2$, where $\hat{\gamma}_1$ and $\hat{\gamma}'_1$ operate on kets with subscript 1 and $\hat{\gamma}_2$ and $\hat{\gamma}'_2$ operate on kets with subscript 2. P_L, P_R denote the fermionic parity of the left and right subsystem of the initial state, respectively. Majorana modes represented by γ_1 and γ_2 are braided around each other adiabatically via a sequence Majorana moves involving a third Majorana pair as shown. For example, the configuration in panel (b) is attained from configuration in panel (a) by adiabatically decreasing the tunneling strength between Majorana modes γ_3 and γ'_3 and at the same time increasing the tunneling strength between γ_3 and γ_2, which effectively leads to γ_2 moving to the new position as shown by the arrow in (b). Assuming the system remains in the ground state throughout the braiding process, the braiding is

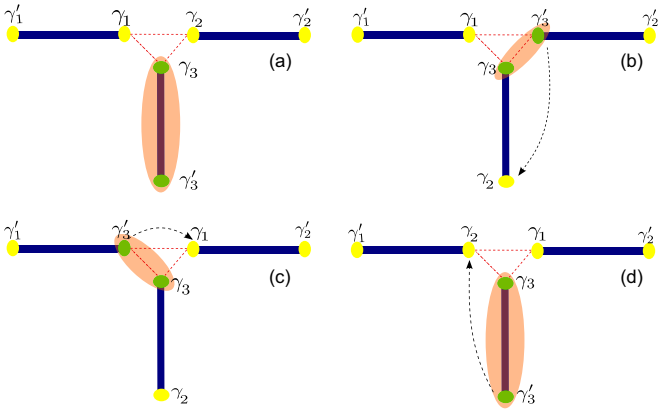

FIG. 9. A schematic diagram for braiding a pair of Majoranas using a trijunction. The system is initialized (a) such that γ'_1, γ_1, γ'_2, and γ_2 are four localized Majorana modes and (γ'_3,γ_3) Majorana pair is paired into a Dirac fermion. Paired Majorana modes are depicted as green discs paired by enhanced wave-function overlap over the region depicted by pink oval. At every move an unpaired Majorana mode is moved from one position to another. The movement of the Majorana resulting from the move resulting in each configuration (b)–(d) is shown by a dashed arrow.

accomplished by the unitary operator

$$U_{12} = \exp\left(\pm\frac{\pi}{4}\hat{\gamma}_1\hat{\gamma}_2\right), \tag{14}$$

where $+/-$ sign in the unitary operator depends on the microscopic details of the system [64]. Considering a more complicated setup one could imagine braiding any two Majoranas independently of the other two. The unitary operators affecting the braiding operation between any two Majoranas do not form a commuting set. Hence MZMs are said to have non-Abelian braiding statistics which offers immense potential for topological quantum computation [17,24].

However, any realistic braiding experiment must take into account a few prominent departures from the idealized set of implicit assumptions made above in our schematic description of perfect Majorana braiding. First, any finite system hosting MZMs will have a finite Majorana wave-function overlap, splitting the Majorana modes by an energy δ, away from zero energy due to the hybridization between the two MZM wave functions from the two wire ends [34]. Obviously, a large overlap (as would happen in shorter nanowires or in systems with small superconducting gaps leading to large coherence lengths) would completely destroy all non-Abelian topological properties since the Majorana excitations in that situation are simply the electron-hole quasiparticle excitations of the superconducting nanowire with the Majorana splitting being comparable to the superconducting energy gap. Including this Majorana splitting in the formalism is an important ingredient of our theory. Second, "adiabatic" braiding process takes place over a finite time scale δt_B (i.e., with a finite braiding velocity), which is associated with the energy uncertainty of the system δE_B by

$$\delta t_B \delta E_B \sim \hbar. \tag{15}$$

We note that this braiding-induced energy uncertainty δE_B must be much larger (smaller) than the Majorana splitting

(superconducting gap) for the braiding operation to manifest any topological non-Abelian behavior. One can loosely identify this energy uncertainty as an effective dissipation term arising from the finite velocity braiding process. Including an energy broadening or a dissipative term is a key ingredient of our theory. Such dissipation could arise from the energy uncertainty associated with braiding as discussed above, but in the specific context of the tunneling conductance measurements, it arises from intrinsic dissipation of strength Γ, which might be present in the experimental situation. In the case of braiding, we will refer to this intrinsic dissipation as Γ' and use Γ to represent the total effective dissipation $\Gamma = \Gamma' + \delta E_B$, that also includes the energy uncertainty δE_B. Note that Γ is finite in the braiding process even when intrinsic dissipation (i.e., Γ') is absent since δE_B is necessarily finite. One may think that it is in principle possible to make δE_B vanish by carrying out the braiding process infinitely slowly (i.e., $\delta E_B = 0$), but this is not allowed (even as a matter of principle) since the Majorana splitting is always finite in any finite wire, and δE_B must always surpass Majorana splitting for the system to act non-Abelian. This is equivalent to our earlier statement that a finite wire can never have a true Majorana-induced zero-bias conductance peak because of Majorana splitting, and the presence of various energy broadening mechanisms (e.g., dissipation, temperature, coupling to the leads) is essential in producing the ZBCP in finite wires even in the nominal topological phase. Thus braiding success and ZBCP are conceptually connected with dissipation playing a central role.

While one might argue that braiding experiments differ fundamentally from conductance experiments since the latter depends on Γ_L and the former does not, the existing braiding proposals [51–65] requires the presence of Majorana fermion tunneling in a key way. The Majorana tunneling enters through the trijunctions in the Majorana braiding proposals. In fact, the energy gap (i.e., Majorana splitting) between Majorana modes at the trijunction is generated by tunneling and takes the place of the tunnel broadening Γ_L in the conductance experiment. Thus inclusion of energy broadening $\Gamma \sim \delta E_B + \Gamma'$ (to represent finite braiding velocity as well as any intrinsic broadening), tunneling broadening Γ_L, and Majorana splitting δ are essential ingredients in the braiding process as much as they are in the tunnel conductance experiments. The TV calculations discussed in the last section thus are fundamentally relevant to the braiding experiments as they are to the conductance experiments since braiding is an operational way of measuring the TI of the system, which we have argued gets converted to TV in finite wires with dissipation.

Let us now discuss if the qualitative dependence of the braiding properties on the parameters (Γ,Γ_L,δ) is similar to their counterparts in the case of conductance. Analogous to the tunneling case, the proper topological movement of MZMs (i.e., the MZMs remaining localized on the time-scale of the braiding operation) requires that the velocity-induced broadening of Majoranas satisfy $\delta \ll \Gamma$ since any braiding must involve an actual physical movement of MZMs around each other. Similarly, Γ_L limits the speed of braiding so that for sucessful braiding we require $\Gamma_L \gg \Gamma = (\delta E_B + \Gamma')$. Furthermore, to ensure the presence of MZMs at the ends of the topological set-up, the finite-size Majorana splitting δ must be smaller than broadening, i.e., $\Gamma_L \gg \delta$. We have assumed here (for the sake of this discussion without any loss of generality) that we are deep in the topological phase so that all parameters $(\Gamma_L,\Gamma,\delta) \lesssim \Delta$, i.e., the topological gap is large, which is necessary for adiabaticity in braiding any way.

We therefore see a one-to-one correspondence between the parameters determining braiding and tunneling measurements with the TV showing up in both measurements as the key quantity determining the topological behavior of the circuit. The braiding properties of the system might be characterized by P_{braid}, which we define to be the probability of success of non-Abelian braiding. The probability of successful non-Abelian braiding, directly related to the TV discussed in the last section, is a function of the amount of nonuniversal broadening Γ present in the braiding experiment (i.e., the sum of the energy uncertainty δE_B and the intrinsic broadening due to coupling to the environment Γ'), the Majorana splitting (δ), the tunnel coupling Γ_L and the topological gap (Δ). Furthermore, since braiding is presumably a topological property, we expect the probability of success of braiding to be determined by the TV since the topological phase for the infinite system is defined by the TI.

Based on these considerations we conjecture that the success rate of non-Abelian braiding for a given braiding speed in an experiment (P_{braid}) is related to probability of TV being -1 (or very close to it), i.e.,

$$P_{\text{braid}}(\delta E_B + \Gamma',\Gamma_L,\delta,\Delta) \sim \frac{1 - \langle Q(\Gamma,\Gamma_L,\delta,\Delta)\rangle}{2}, \qquad (16)$$

where $\langle Q\rangle$ is the average of TV over disorder realizations for a given disorder strength, and Γ' is the environment-induced intrinsic broadening in the braiding experiment. Γ_L in a tunneling conductance experiment represented in the RHS of Eq. (16) is the lead broadening as discussed in the previous sections. However, Γ_L appearing in the LHS of Eq. (16) represents the induced tunnel gap as a result of strongly coupled adjacent Majorana modes forming a Dirac fermion (strong Majorana pairing regions depicted by pink ovals in Fig. 9). The role played by lead induced broadening for conductance experiment is now played by the energy gap induced by coupling adjacent nanowire edge modes forming a Dirac fermion in the braiding experiment, and therefore for the sake of brevity, we have chosen to represent it with the same symbol Γ_L on both sides of Eq. (16) although the Γ_L appearing in conductance and braiding experiments arises from different tunneling mechanisms.

From the previous section, we know that whether the average TV $\langle Q\rangle$ is nearly topological (i.e., a negative number with magnitude close to unity), which [according to our conjecture Eq. (16)] would correspond to successful braiding, is directly correlated with the presence of a ZBCP value close to the topological value $G(V \sim 0) \sim G_0$. Such a nearly quantized ZBCP, which can be tested for through existing experimental setups [1,8,10–13], can only occur in a much smaller parameter regime $\Delta \gg \Gamma_L \gg \Gamma \gg \delta$. Furthermore, temperature, which provides a fifth independent energy scale through the thermal energy k_BT (which we take to be zero) must be small as well. It is only in this topological parameter regime that one expects braiding to be reasonably successful. We believe that this parameter regime can be diagnosed from

the much simpler conductance quantization measurements carried out on the same or similar samples (i.e., with similar values of Γ and Γ_L in both cases).

Our results (see Fig. 5) in Sec. IV indicate that a ZBCP value around half of the quantized value (i.e., ZBCP $\sim e^2/h$) should be adequate to produce a negative TV value. The negative TV would correpond to the topologically nontrivial phase with a TI of -1. Based on this, we conclude that braiding experiments would succeed (perhaps with rather low visibility) as long as the corresponding ZBCP is around e^2/h (or larger) in the same nanowire sample with identical system parameters. We believe that for systems with ZBCP much lower than e^2/h, the braiding experiments are unlikely to succeed in manifesting a purely topological phase with a TV value of -1. This is an important predicted experimental consequence of our theory. We therefore believe that braiding measurements should only be attempted on nanowire samples with the largest possible ZBCP values, and perhaps, braiding in samples with ZBCP values much lower than e^2/h is unlikely to manifest non-Abelian statistics (even with low visibility—see our Fig. 5).

V. CONCLUSION

In this work, we ask whether a theoretical connection can be established between the tunneling conductance and the topological visibility of realistic spin-orbit coupled semiconductor nanowires in the presence of proximity induced superconductivity and Zeeman splitting, assuming the system parameters (Zeeman splitting, chemical potential, superconducting energy gap) to be in the topological phase so that the wire carries Majorana zero modes localized at the wire ends. The question takes on special significance because of the putative non-Abelian braiding properties of MZMs enabling fault tolerant quantum computation. In particular, direct braiding experiments, which are typically very hard, establishing the non-Abelian nature of MZMs have not yet been carried out in semiconductor nanowires although many proposals to do so exist in the theoretical literature. [Such experiments do exit in the fractional quantum Hall context for the so-called 5/2 fractional quantum Hall state, but the results are difficult to interpret and have remained controversial (see Ref. [82] and references therein).] On the other hand, several groups have carried out tunneling conductance measurements in semiconductor nanowires following specific theoretical predictions that MZMs should manifest as zero-bias conductance peaks in such experiments. The observation of such ZBCPs has so far been hailed as the evidence for the predicted existence of MZMs in these nanowires, but doubts remain about how topological such systems are (even if the observed ZBCP signal indeed arises from MZM-related physics and is not some spurious effect), particularly in view of the disturbing fact that the measured ZBCP values are substantially lower than the quantized conductance value (i.e., $2e^2/h$) expected from the perfect Andreev reflection by the Majorana modes. Even assuming that the system is in the topological phase as far as parameter values go, serious issues arise from the finite length of the wires, which, coupled with the expected long coherence length because of the small induced superconducting gap [83], leads to questions regarding the overlap between the MZMs localized at the two wire ends. Such MZM hybridization would lead to large Majorana energy splittings, and the MZMs would be shifted from zero-energy, becoming instead finite energy resonances in the gap. If the Majorana energy splitting is comparable to the energy gap itself, then obviously there can be no non-Abelian braiding statistics since these split Majorana modes are essentially electron-hole pairs. The quantitative technical question now becomes whether such approximate (or almost)- MZMs, which are split and thus shifted from zero energy, could still lead to non-Abelian statistics although the ZBCP associated with them is below the quantized conductance $2e^2/h$. We address this question in great detail by calculating both the tunnel conductance and the TV of the same realistic nanowire (i.e., using exactly the same parameter values) and comparing them carefully.

The TV in the ideal situation is $+/-1$ with the negative (positive) sign corresponding to the topological (trivial) phase, just as the tunnel conductance in the ideal situation is $2e^2/h$ (0) for the topological (trivial) phase. But, in real measurements, the existence of Majorana splitting in finite wires plus various dissipative broadening mechanisms invariably present in real systems could lead to a value of the TV with a magnitude less than unity, just as the ZBCP magnitude could be less than $2e^2/h$ from the same physics. Correlating the two quantities in realistic wires would tell us whether braiding experiments are likely to succeed in realistic nanowires currently being studied in various laboratories. One aspect regarding Majorana nanowires is that a naive calculation of the ZBCP in the presence of Majorana splitting in finite wires always leads to zero conductance at zero energy since the finite energy split Majorana resonances have no spectral weight at zero energy. This of course changes in the presence of any energy broadening which must invariably be present in real systems. This is quite analogous to the situation of purely adiabatic braiding, where braiding at a rate much smaller than the Majorana splitting δ would also produce purely nontopological results. Our work explicitly includes this energy broadening effect in order to comment on real systems of experimental interest. We believe that our calculated TV in realistic systems provides the actual visibility of future braiding measurements through the inclusion of broadening processes, i.e., our finding a TV differing in magnitude from unity has one to one correspondence with the corresponding averaged braiding experiment runs over many measurements (where the average will differ from unity in magnitude although each run itself will give a value of $+/-1$). We note that indeed the calculated TV is negative or positive (but always < 1 in magnitude), depending on whether the system is approximately topological or trivial, respectively. The exact value of our calculated topological visibility predicts the outcome of braiding experiments—closer our results are to -1 more non-Abelian is the system, but any negative value for the topological visibility could be construed as predicting the system to be in the non-Abelian topological phase, albeit with a low visibility if the value of the topological visibility is far from -1. On the other hand, our finding of a positive topological visibility indicates that the corresponding system is nontopological.

Our work shows that the topological quantum phase transition separating the trivial phase (a TV value of 1 and a ZBCP value of zero) from the topological phase (a TV value of -1 and a ZBCP value of $2e^2/h$) is a crossover in real systems (even at zero temperature) because of the presence of the broadening terms Γ, tunneling Γ_L and the Majorana splitting

(δ). The inclusion of the dissipative broadening processes, which must invariably be present in real systems, is a key ingredient of our theory—in fact, without any broadening, the ZBCP is always zero at zero energy by virtue of the Majorana splitting in all finite wires. We find that the ZBCP evolves from a quantized peak deep in the topological phase into a much smaller peak on a large background near the transition, quite similar to some of the experimental results [1,8,10–13]. Unfortunately, the corresponding TV in this case is invariably nontopological as long as the ZBCP value is small. In braiding experiments the broadening is to be interpreted as the energy uncertainly associated with the finite braiding time, which should be large compared with the Majorana splitting for braiding to succeed (i.e., $\Gamma > \delta$ must apply for the TV to be negative). For braiding to succeed, of course, one must always be deep in the topological gap so that the topological gap is much larger than the Majorana splitting (δ), and intrinsic broadening (Γ). Furthermore, the Majorana coupling energy Γ_L must be large enough to overcome the splitting δ to lead to a large conductance and also for the trijunctions in a braiding protocol to lead to non-Abelian statistics.

We find that it is possible for the system to be topological (i.e., negative value for the TV) even when the corresponding zero-bias conductance value is suppressed from $2e^2/h$—in particular, a factor of 2 suppression of the ZBCP would still lead to the existence of non-Abelian braiding statistics (with somewhat low visibility). On the other hand, we believe that systems with ZBCP values factors of 10 (or more) suppressed from $2e^2/h$ are unlikely to ever manifest non-Abelian statistics, and such systems are better considered as nontopological systems because of the very large Majorana splitting in spite of there being a small ZBCP peak. Our most important qualitative conclusion is the finding that it is indeed possible for a finite wire with split MZMs (and a correspondingly suppressed ZBCP value compared with $2e^2/h$) to manifest non-Abelian braiding statistics with the visibility of braiding (averaged over many runs) decreasing with decreasing value of the corresponding ZBCP. How small the ZBCP can be and still reflect an underlying non-Abelian braiding statistics depends on many details (most importantly the ratio of the Majorana splitting energy to the topological gap which should typically be less than 0.2 for braiding to succeed) including the energy broadening in the system arising from many nonuniversal mechanisms. One important conclusion following from our extensive numerical simulations is that braiding experiments are perhaps likely (unlikely) to succeed in nanowires manifesting ZBCP values at least around e^2/h (much less than e^2/h) since we find that the calculated topological visibility crosses over from being negative to positive for the corresponding tunneling ZBCP value crossing over respectively from being $>e^2/h$ to being $<e^2/h$. Of course, real braiding experiments would obviously not be carried out in the tunneling configurations with leads to normal contacts for measuring tunneling currents, but our results indicate that braiding should focus on nanowires manifesting ZBCP values not much less than e^2/h for a reasonable chance of any success in the observation of non-Abelian braiding statistics. We mention that braiding experiments still involve aspects of tunneling (i.e., a finite Γ_L), which must arise from the finite Majorana tunneling at wire junctions (in contrast to NS junctions in the conductance measurements) necessary to make the MZMs go around each other in order to accomplish braiding.

Finally, we note that we have neglected finite temperature and disorder effects in our theory, assuming clean nanowires at zero temperature in order to consider the best case scenarios. We have assumed zero temperature for simplicity and to avoid introducing extra parameters, even though it is rather simple to introduce finite temperature effects into the conductance calculations. This is because finite temperature conductance of a noninteracting system can be obtained simply by broadening the conductance traces by a fermi function. The result of such a broadening is easy to surmise from the zero temperature plot. The most important effect of introducing temperature would be to potentially suppress the zero-bias conductance peak and generally eliminate sharp features, quite similar to the broadening Γ that we have introduced. However, this is significant only if the temperature T is large enough (i.e., $T \gtrsim \Gamma$). This limit is easy to detect in experiments since the width of the peak should correspond to temperature. Therefore our results focus on the limit where temperature is low enough so as to be smaller than the width of the peak as in the recent experiments [35]. Additionally, finite temperature does not invalidate our conjecture regarding braiding since T must also be smaller than Γ_L (related to the gap) for successful braiding. Since nanowire conductance and braiding experiments are carried out at very low temperatures ($\sim$20$-$50 mK) any way, our neglect of finite temperature is not a serious problem. Including disorder effects is also straightforward and only increases the computational time substantially (without introducing any theoretical complications), which is why they are left out. We emphasize that our conclusion remains completely unaffected by finite temperature and disorder. Finite temperature only reduces the visibility, thus further reducing the magnitude of the ZBCP and the TV, without affecting the topological or not question at all. Thus the braiding experiment should be performed at the lowest possible temperatures to maximize the visibility. Disorder complicates matters only because it shifts the condition for obtaining the topological phase (i.e., the TPT point), but it cannot affect the basic physics at all since the induced topological superconductivity arises from an interplay among the s-wave superconductivity, spin-orbit coupling, and Zeeman splitting—all of which are immune to disorder. The fact that disorder does not suppress the topological phase (but does shift its location on the phase diagram compared with the clean parameters) is already well-known in the literature [67], and we therefore refrain from providing finite disorder results since this will only complicate the presentation with no additional conceptual or theoretical understanding. The situation with very strong disorder is, however, disastrous for the manifestation of topological properties since the strongly disordered nanowire will manifest Griffiths phase physics with many MZMs localized randomly along the wire [70,80], and this situation must obviously be avoided at all costs for all braiding experiments. We have ensured numerically that all our conclusions in this paper remain unaffected in the presence of finite temperature and (weak) disorder as asserted above. Similarly, multisubband occupancy of the nanowire [84,85] does not change any of our conclusions either, as long as an odd number of spin-split subbands are occupied in the system,

and the appropriate microscopic parameters (i.e., δ, Γ, Γ_L, Δ, chemical potential) are all modified to take into account the multisubband occupancy in the nanowire. Of course, the relative values of the various parameters may be modified by multisubband occupancy, which must be incorporated in the theory appropriately, but the theory itself remains exactly the same as long as an odd number of subbands are occupied in the nanowire and various parameters are appropriately modified to reflect the multisubband occupancy of the system.

The new important concept introduced in this work is of topological visibility, which is essentially the "nonunitary" version of the well-known "topological invariant" extensively used to characterize topological superconductivity. Whereas the topological invariant is a topological index, being $+1$ or -1 corresponding to trivial and topological superconductors respectively, the topological visibility by contrast corresponds to a continuous variable (varying between $+1$ and -1) relevant for finite systems where a naive computation of the topological invariant will always indicate a trivial phase by virtue of the Majorana energy splitting always being finite in finite systems. The topological visibility is a physical (and practical) generalization of the mathematical concept of topological invariant to realistic finite nanowires in the laboratory, where some Majorana splitting is inevitable because of the wave-function overlap between the Majorana zero modes localized at the two ends of the finite wire. The physical mechanism enabling the existence of topological visibility is dissipation or level broadening invariably present in all real systems. In particular, this broadening must exceed the Majoana energy splitting for the system to behave "topologically" (i.e., for the topological visibility to be negative). However, this dissipative broadening also suppresses the value of ZBCP below the canonically quantized value of $2e^2/h$ in the topological phase and reduces the magnitude of the topological visibility below unity. For braiding experiments of the future, a part of this dissipation arises from the finite speed of braiding itself which gives rise to an energy broadening, and this broadening must exceed the Majorana splitting energy for the system to behave as a non-Abelian system. Although our numerical results (when compared with tunnel conductance measurements) indicate that some dissipative broadening must be present in the real systems, we do not investigate in the current work the possible physical mechanisms producing such dissipation. At this stage, our inclusion of dissipative broadening in the theory is phenomenological, and future experiments will have to determine the source of such broadening in real systems. One possibility is that the combination of disorder and magnetic field in the s-wave superconductor leads to subgap fermionic states at the interface. Such subgap fermionic states, at finite temperature and in the presence of electron phonon coupling can lead to the creation of a fermion bath that would have the same form assumed in this paper.

ACKNOWLEDGMENTS

This work is supported by Microsoft Q, LPS-MPO-CMTC, and JQI-NSF-PFC. We acknowledge valuable discussions with L. Kouwenhoven.

APPENDIX A: TUNNELING CONDUCTANCE AND TOPOLOGICAL VISIBILITY FROM *S* MATRIX

Tunneling conductance is a local measurement at the normal lead-superconducting nanowire (see Fig. 1) junction, and one may calculate it theoretically by assuming both the lead and nanowire to extend semi-infinitely and coupled together at the so-called normal metal-superconductor (NS) junction via a tunnel barrier.

The knowledge of the reflection matrix at the NS junction is sufficient to calculate the tunneling conductance. The reflection matrix has the form

$$r = \begin{pmatrix} r_{ee} & r_{eh} \\ r_{he} & r_{hh} \end{pmatrix}, \tag{A1}$$

where r_{ee} and r_{eh} are the normal and Andreev reflection amplitudes, respectively. Here, the reflection matrix is expressed in the basis of electron and hole scattering channels, which is called the particle-hole basis. Such a convenient decomposition in normal and Andreev reflection amplitudes is possible whenever the lead Hamiltonian, $H_{\rm lead}$ [see Eq. (7)], is diagonal in the particle hole basis, i.e., $[H_{\rm lead}, \tau_z] = 0$. For a single conducting channel, the tunneling conductance to a superconductor in the NS junction is given by the Blonder-Tinkham-Klapwijk (BTK) formula [86] (in the units of e^2/h)

$$G = 1 - |r_{ee}|^2 + |r_{eh}|^2. \tag{A2}$$

With N conducting modes in the lead, r_{ee} and r_{eh} acquire a matrix structure, and the BTK formula is generalized to

$$G = N - \mathrm{Tr}(r_{ee} r_{ee}^\dagger - r_{eh} r_{eh}^\dagger).$$

For a periodic translationally invariant spinless p-wave superconductor described by a Hamiltonian $H(k)$ in k space, Kitaev [14] defined the TI as

$$Q_{\rm Kitaev} = \mathrm{sgn}(\mathrm{Pf}(iH(0))\mathrm{Pf}(iH(\pi))), \tag{A3}$$

where Pf denotes Pfaffian operation on a matrix. $Q_{\rm Kitaev} = -1$ implies that the system is in a topological phase, i.e., if the same Hamiltonian were to describe a finite chain with an open boundary condition, the system edges will host non-Abelian Majorana zero modes. For an open finite wire geometry, Akhmerov *et al.* [66] provided the following generalization for the TI in terms of the reflection matrix:

$$Q_0 = \mathrm{sgn}(\det(r)). \tag{A4}$$

It was argued in the main body of the paper that in presence of dissipation, a more useful quantity to characterize topological properties of the system is TV—a quantity closely related to scattering matrix TI (A4), defined as

$$Q = \det(r). \tag{A5}$$

To justify this expression for the TV, which we use in our numerical work, consider the particle-hole symmetry of the superconducting Bogoliubov-de Gennes (BdG) Hamiltonian, i.e.,

$$\Pi H_{\rm BdG} \Pi^{-1} = -H_{\rm BdG}, \tag{A6}$$

where $\Pi = \tau_x C$ with C being the complex conjugation operator. This leads to the following constraint on the reflection

matrix:

$$\tau_x r \tau_x = r^*, \tag{A7}$$

which implies

$$\det(r) = \det(r)^*. \tag{A8}$$

Note that we have implicitly assumed the voltage bias V to be zero. For finite V, the particle-hole constraint on the voltage-dependent reflection matrix $r(V)$ takes the form $\tau_x r(V)\tau_x = r(-V)^*$. When the voltage bias is less than the superconducting gap ($eV < \Delta$), the transmission through the nanowire is zero as there are no extended states. Therefore the reflection matrix r is unitary, i.e., $rr^\dagger = 1$. This implies

$$\mathrm{Tr}(r_{ee}r_{ee}^\dagger + r_{eh}r_{eh}^\dagger) = \mathrm{Tr}(r_{hh}r_{hh}^\dagger + r_{he}r_{he}^\dagger) = N, \tag{A9}$$

and that the absolute value of the determinant of reflection matrix satisfies

$$|\det(r)| = 1. \tag{A10}$$

Combined with the particle-hole symmetry constraint of r, we get $\det(r) = \pm 1$. In other words, we have shown that whenever reflection matrix r respects unitarity and particle-hole symmetry, the TI [defined as $\mathrm{sgn}(\det(r))$] is equal to TV [defined as $\det(r)$], i.e., $Q_0 = Q$. An ideal system with MZMs is characterized by $\det(r) = -1$ [and nontopological trivial phase is characterized by $\det(r) = 1$] and also is associated with quantized ZBCP at $2e^2/h$. The only way to change the value of $\det(r)$ is to break the unitarity by closing the topological gap. Note that by substituting Eq. (A9) in Eq. (A3) and using the unitarity of the reflection matrix one can show

$$G = 2\mathrm{Tr}(r_{eh}r_{eh}^\dagger), \tag{A11}$$

$$\mathrm{Tr}(r_{eh}r_{eh}^\dagger) = \mathrm{Tr}(r_{he}r_{he}^\dagger). \tag{A12}$$

Moreover, particle-hole symmetry of r implies

$$r_{eh}(V) = r_{he}^\dagger(-V). \tag{A13}$$

Finally, using Eqs. (A13) and (A12), we arrive at

$$G(V) = G(-V). \tag{A14}$$

So the unitarity and particle-hole symmetry of r guarantee that the in-gap conductance is symmetric about zero bias. For a finite system, any MZM would be split in energy by δ because of the inevitable MZM overlap from the two ends (which could be exponentially small, but never zero for a finite wire). Strictly, at zero energy, there would be no BdG eigenstate in the nanowire rendering an incoming electron to be totally reflected with $\det(r) = 1$. We would infer, based on this argument, that all finite systems irrespective of whether they host MZMs or not are nontopological. This is similar to the statement in an entirely different context that no finite system can have a phase transition, which is only a property of the infinite volume thermodynamic limit. In reality, other (nonuniversal) cutoffs in energy and length scales of the problem become important as the system size increases, and eventually finite and infinite systems behave in the same manner. For the nanowire MZM problem, this arises from the energy broadening inherent in any realistic system, which renders the split hybridized non-zero-energy peaks into a broadened midgap peak with a finite weight at zero energy. Thus the split resonances at sharp nonzero energies become a broad peak around zero energy with a finite width. Without such a dissipative broadening process, the splitting of the MZMs invariably present in any real system with finite wire length will always lead to precisely zero conductance at zero energy since the MZMs are now always shifted from zero energy due to Majorana splitting.

We account for finite lifetime of the quasiparticle due to various inelastic scattering mechanisms such as phonons and magnetic moments through an onsite imaginary term in the Hamiltonian. We emphasize that without this broadening, a finite wire can never have a true zero-energy mode, and the system is by definition always in the trivial phase! The resultant broadening due to the onsite imaginary term in the Hamiltonian is given by Γ.

APPENDIX B: NUMERICAL CALCULATION OF TOPOLOGICAL VISIBILITY

To calculate the TV, we numerically compute the real part of the determinant of the reflection matrix r and discard the small imaginary part of the determinant, which is a numerical artifact as can be seen from the fact that the particle-hole symmetry forces the determinant of the reflection matrix to be real, which was pointed out in Appendix A. For all calculations involving the leads, the following set of parameters are chosen: $\mu_o B_{\mathrm{lead}} = 2$ K and $\mu_{\mathrm{lead}} = 6.9$ K.

Special care must be taken in calculating the TV. When the submatrices of the reflection matrix (r_{ee}, r_{eh}, r_{he}, and r_{hh}) are called in KWANT, the individual submatrix outputs do not satisfy the particle-hole constraint given by Eq. (A7). The particle-hole symmetry was restored in the following way in our calculations. Since the lead parameters were chosen to have two incoming and two outgoing modes at zero energy, in every lead for each participating mode m_1,m_2 at zero energy, incoming and outgoing wave functions have a generic two component structure

$$\Psi = \begin{pmatrix} \psi_1 \\ \psi_2 \end{pmatrix}.$$

We compute $\alpha = \max(\psi_1, \psi_2)$ at the end site of the lead and define the phase of the wave function to be $\phi = \alpha/|\alpha|$. The arbitrary phase of the reflection matrix is rectified by multiplying $\det(r)$ by the following string of phases:

$$\phi_{in,e}^{m_1}\phi_{in,e}^{m_2}\phi_{in,h}^{m_1}\phi_{in,h}^{m_2}\phi_{out,e}^{m_1}\phi_{out,e}^{m_2}\phi_{out,h}^{m_1}\phi_{out,h}^{m_2}, \tag{B1}$$

where in and out stand for incoming and outgoing modes, e and h stand for electron and hole, and m_1 and m_2 are the two modes. These subtle numerical manipulations are essential in ensuring that the mode functions used by KWANT are particle-hole symmetric. The particle-hole symmetry of the basis is key to ensure the particle-hole symmetry of the scattering matrix that is required for the proper evaluation of the scattering matrix topological visibility.

[1] V. Mourik, K. Zuo, S. M. Frolov, S. R. Plissard, E. P. A. M. Bakkers, and L. P. Kouwenhoven, Science **336**, 1003 (2012).
[2] Jay D. Sau, Roman M. Lutchyn, Sumanta Tewari, and S. Das Sarma, Phys. Rev. Lett. **104**, 040502 (2010).
[3] Roman M. Lutchyn, Jay D. Sau, and S. Das Sarma, Phys. Rev. Lett. **105**, 077001 (2010).
[4] Jason Alicea, Phys. Rev. B **81**, 125318 (2010).
[5] Jay D. Sau, S. Tewari, Roman M. Lutchyn, Tudor D. Stanescu, and S. Das Sarma, Phys. Rev. B **82**, 214509 (2010).
[6] Y. Oreg, G. Refael, and Felix von Oppen, Phys. Rev. Lett. **105**, 177002 (2010).
[7] X. Liu, J. D. Sau, and S. Das Sarma, Phys. Rev. B **92**, 014513 (2015).
[8] M. T. Deng, C. L. Yu, G. Y. Huang, M. Larsson, P. Caroff, and H. Q. Xu, Nano Lett. **12**, 6414 (2012).
[9] Leonid P. Rokhinson, Xinyu Liu, and Jacek K. Furdyna, Nat. Phys. **8**, 795 (2012).
[10] Anindya Das, Yuval Ronen, Yonatan Most, Yuval Oreg, Moty Heiblum, and Hadas Shtrikman, Nat. Phys. **8**, 887 (2012).
[11] A. D. K. Finck, D. J. Van Harlingen, P. K. Mohseni, K. Jung, and X. Li, Phys. Rev. Lett. **110**, 126406 (2013).
[12] H. O. H. Churchill, V. Fatemi, K. Grove-Rasmussen, M. T. Deng, P. Caroff, H. Q. Xu, and C. M. Marcus, Phys. Rev. B **87**, 241401 (2013).
[13] W. Chang, S. M. Albrecht, T. S. Jespersen, F. Kuemmeth, P. Krogstrup, J. Nygrd, and C. M. Marcus, Nat. Nanotechnol. **10**, 232 (2015).
[14] Alexei Kitaev, Phys. Usp. **44**, 131 (2001).
[15] K. Sengupta, I. Zutic, H.-J. Kwon, V. M. Yakovenko, and S. Das Sarma, Phys. Rev. B **63**, 144531 (2001).
[16] K. T. Law, P. A. Lee, and T. K. Ng, Phys. Rev. Lett. **103**, 237001 (2009).
[17] Chetan Nayak, Steven H. Simon, Ady Stern, Michael Freedman, and S. Das Sarma, Rev. Mod. Phys. **80**, 1083 (2008).
[18] Jason Alicea, Rep. Prog. Phys. **75**, 076501 (2012).
[19] C. W. J. Beenakker, Annu. Rev. Con. Mat. Phys. **4**, 113 (2013).
[20] M. Leijnse and K. Flensberg, Semicond. Sci. Technol. **27**, 124003 (2012).
[21] S. R. Elliott and M. Franz, Rev. Mod. Phys. **87**, 137 (2015).
[22] T. D. Stanescu and S. Tewari, J. Phys. Condens. Matter **25**, 233201 (2013).
[23] S. Das Sarma, M. Freedman, and C. Nayak, Phys. Today **59**, 32 (2006).
[24] S. Das Sarma, M. Freedman, and C. Nayak, Npj Quantum Information **1**, 15001 (2015).
[25] D. Bagrets and A. Altland, Phys. Rev. Lett. **109**, 227005 (2012).
[26] P. Neven, D. Bagrets, and A. Altland, New J. Phys. **15**, 055019 (2013).
[27] Eduardo J. H. Lee, X. Jiang, M. Houzet, R. Aguado, Charles M. Lieber, and S. De Franceschi, Nat. Nano **9**, 79 (2013).
[28] F. Pientka, G. Kells, A. Romito, P. W. Brouwer, and F. von Oppen, Phys. Rev. Lett. **109**, 227006 (2012).
[29] G. Kells, D. Meidan, and P. W. Brouwer, Phys. Rev. B **85**, 060507 (2012).
[30] Jie Liu, Andrew C. Potter, K. T. Law, and Patrick A. Lee, Phys. Rev. Lett. **109**, 267002 (2012).
[31] D. I. Pikulin, J. P. Dahlhaus, M. Wimmer, H. Schomerus, and C. W. J. Beenakker, New J. Phys. **14**, 125011 (2012).
[32] K. Flensberg, Phys. Rev. B **82**, 180516 (2010).
[33] M. Wimmer, A. R. Akhmerov, J. P. Dahlhaus, and C. W. J. Beenakker, New J. Phys. **13**, 053016 (2011).
[34] C.-H. Lin, J. D. Sau, and S. Das Sarma, Phys. Rev. B **86**, 224511 (2012).
[35] H. Zhang, Ö. Gül, S. Conesa-Boj, K. Zuo, V. Mourik, F. K. de Vries, J. van Veen, D. J. van Woerkom, M. P. Nowak, M. Wimmer *et al.*, arXiv:1603.04069.
[36] M. Cheng, R. M. Lutchyn, V. Galitski, and S. Das Sarma, Phys. Rev. Lett. **103**, 107001 (2009).
[37] M. Cheng, R. M. Lutchyn, V. Galitski, and S. Das Sarma, Phys. Rev. B **82**, 094504 (2010).
[38] D. Rainis, L. Trifunovic, J. Klinovaja, and D. Loss, Phys. Rev. B **87**, 024515 (2013).
[39] S. Das Sarma, Jay D Sau, and Tudor D Stanescu, Phys. Rev. B **86**, 220506 (2012).
[40] S. Takei, B. M. Fregoso, H.-Y. Hui, A. M. Lobos, and S. Das Sarma, Phys. Rev. Lett. **110**, 186803 (2013).
[41] J. D. Sau, S. Das Sarma, Phys. Rev. B. **88**, 064506 (2013).
[42] P. W. Brouwer, M. Duckheim, A. Romito, and F. von Oppen, Phys. Rev. B **84**, 144526 (2011).
[43] P. W. Brouwer, M. Duckheim, A. Romito, and F. von Oppen, Phys. Rev. Lett. **107**, 196804 (2011).
[44] E. Prada, P. San-Jose, and R. Aguado, Phys. Rev. B **86**, 180503 (2012).
[45] D. Chevallier, P. Simon, and C. Bena, Phys. Rev. B **88**, 165401 (2013).
[46] C. M. Marcus (unpublished).
[47] A. M. Lobos and S. Das Sarma, New J. Phys. **17**, 065010 (2015).
[48] B. M. Fregoso, A. M. Lobos, and S. Das Sarma, Phys. Rev. B **88**, 180507 (2013).
[49] N. Read and D. Green, Phys. Rev. B **61**, 10267 (2000).
[50] D. A. Ivanov, Phys. Rev. Lett. **86**, 268 (2001).
[51] J. Alicea, Y. Oreg, G. Refael, F. von Oppen, and M. P. A. Fisher, Nat. Phys. **7**, 412 (2011).
[52] J. D. Sau, S. Tewari, and S. Das Sarma, Phys. Rev. B **84**, 085109 (2011).
[53] D. J. Clarke, J. D. Sau, and S. Tewari, Phys. Rev. B **84**, 035120 (2011).
[54] T. Hyart, B. van Heck, I. C. Fulga, M. Burrello, A. R. Akhmerov, and C. W. J. Beenakker, Phys. Rev. B **88**, 035121 (2013).
[55] C. S. Amorim, K. Ebihara, A. Yamakage, Y. Tanaka, and M. Sato, Phys. Rev. B **91**, 174305 (2015).
[56] B. Van Heck, A. R. Akhmerov, F. Hassler, M. Burrello, and C. W. J. Beenakker, New J. Phys. **14**, 035019 (2012).
[57] Q.-F. Liang, Z. Wang, and X. Hu, Europhys. Lett. **99**, 50004 (2012).
[58] A. Romito, J. Alicea, G. Refael, and F. von Oppen, Phys. Rev. B **85**, 020502 (2012).
[59] B. I. Halperin, Y. Oreg, A. Stern, G. Refael, J. Alicea, and F. von Oppen, Phys. Rev. B **85**, 144501 (2012).
[60] P. Kotetes, G. Schön, and A. Shnirman, J. Korean Phys. Soc. **62**, 1558 (2013).
[61] D. J. Clarke, J. D. Sau, and S. Das Sarma, Phys. Rev. X **6**, 021005 (2016).
[62] X.-J. Liu and A. M. Lobos, Phys. Rev. B **87**, 060504 (2013).
[63] C.-K. Chiu, M. Vazifeh, and M. Franz, Europhys. Lett. **110**, 10001 (2015).
[64] J. D. Sau, D. J. Clarke, and S. Tewari, Phys. Rev. B **84**, 094505 (2011).

[65] J. D. Sau, S. Tewari, and S. Das Sarma, Phys. Rev. A **82**, 052322 (2010).
[66] A. R. Akhmerov, J. P. Dahlhaus, F. Hassler, M. Wimmer, and C. W. J. Beenakker, Phys. Rev. Lett. **106**, 057001 (2011).
[67] İ. Adagideli, M. Wimmer, and A. Teker, Phys. Rev. B **89**, 144506 (2014).
[68] I. C. Fulga, F. Hassler, A. R. Akhmerov, and C. W. J. Beenakker, Phys. Rev. B **83**, 155429 (2011).
[69] D. I. Pikulin and Y. V. Nazarov, JETP Lett. **94**, 693 (2012).
[70] W. S. Cole, J. D. Sau, and S. Das Sarma, arXiv:1603.03780.
[71] F. L. Pedrocchi and D. P. DiVincenzo, Phys. Rev. Lett. **115**, 120402 (2015).
[72] T. Karzig, G. Refael, and F. von Oppen, Phys. Rev. X **3**, 041017 (2013).
[73] M. Cheng, V. Galitski, and S. Das Sarma, Phys. Rev. B **84**, 104529 (2011).
[74] M. S. Scheurer and A. Shnirman, Phys. Rev. B **88**, 064515 (2013).
[75] T. Karzig, A. Rahmani, F. von Oppen, and G. Refael, Phys. Rev. B **91**, 201404 (2015).
[76] T. Karzig, F. Pientka, G. Refael, and F. von Oppen, Phys. Rev. B **91**, 201102 (2015).
[77] J. D. Sau, S. Tewari, and S. Das Sarma, Phys. Rev. B **85**, 064512 (2012).
[78] C. W. Groth, M. Wimmer, A. R. Akhmerov, and X. Waintal, New J. Phys. **16**, 063065 (2014).
[79] S. Sachdev, *Quantum Phase Transitions* (Cambridge University Press, 2011).
[80] Olexei Motrunich, Kedar Damle, and David A. Huse, Phys. Rev. B **63**, 224204 (2001).
[81] S. Datta, *Electronic Transport in Mesoscopic Systems* (Cambridge University Press, 1997).
[82] R. Willet, Rep. Prog. Phys. **76**, 076501 (2013).
[83] S. Das Sarma, H.-Y. Hui, P. Brydon, and J. D. Sau, New J. Phys. **17**, 075001 (2015).
[84] R. M. Lutchyn, T. D. Stanescu, and S. Das Sarma, Phys. Rev. Lett. **106**, 127001 (2011).
[85] T. D. Stanescu, R. M. Lutchyn, and S. Das Sarma, Phys. Rev. B **84**, 144522 (2011).
[86] G. E. Blonder, M. Tinkham, and T. M. Klapwijk, Phys. Rev. B **25**, 4515 (1982).